Chapter 2

SplicePie: a novel analytical approach for the detection of alternative, non-sequential and recursive splicing

I.Pulyakhina[1], I. Gazzoli[1], P.A.C. ’t Hoen[1], N.E. Verwey[1], J.T. den Dunnen[1,2], A. Aartsma-Rus[1], J.F.J. Laros[1,2]

1 Department of Human Genetics, Leiden University Medical Center, Leiden, the Netherlands
2 Leiden Genome Technology Center, Leiden University Medical Center, Leiden, the Netherlands

Nucleic Acids Research, 2015 Jul 13;43(12):e80. doi: 10.1093/nar/gkv242

2.1 Abstract

Alternative splicing is a powerful mechanism present in eukaryotic cells to obtain a wide range of transcripts and protein isoforms from a relatively small number of genes. The mechanisms regulating (alternative) splicing and the paradigm of consecutive splicing has recently been challenged, especially for genes with a large number of introns. RNA-Seq, a powerful technology using deep sequencing in order to determine transcript structure and expression levels, is usually performed on mature mRNA, therefore not allowing detailed analysis of splicing progression. Sequencing pre-mRNA at different stages of splicing potentially provides insight into mRNA maturation. Although the number of tools that analyze total and cytoplasmic RNA in order to elucidate the transcriptome composition is rapidly growing, there are no tools specifically designed for the analysis of nuclear RNA (which contains mixtures of pre- and mature mRNA). We developed dedicated algorithms to investigate the splicing process. In this paper we present a new classification of RNA-Seq reads based on three major stages of splicing: pre-, intermediate- and post-splicing. Applying this novel classification we demonstrate the possibility to analyze the order of splicing. Furthermore, we uncover the potential to investigate the multi step nature of splicing, assessing various types of recursive splicing events. We provide biological insight into the order of splicing, show that non-sequential splicing of certain introns is reproducible and coinciding in multiple cell lines. We validated our observations with independent experimental technologies and showed the reliability of our method. The pipeline, named *SplicePie*, is freely available online[1]. The example data can also be found online[2].

2.2 Introduction

During messenger RNA (mRNA) splicing, introns are removed and exons are joined to generate a mature mRNA or a transcript. One transcript, usually chosen arbitrarily, to which all other transcripts are compared is called the "reference transcript". The deviations from this standard reference transcript are called alternative transcripts.

Data obtained with recent technologies, such as next generation sequencing (NGS) of a whole transcriptome, revealed that around 90% of human genes undergo alternative splicing [12, 84]. Alternative splicing of a gene comes in different flavours, such as skipping (a part of) an exon [85] or intron retention [86].

Splicing generally occurs cotranscriptionally [87, 88], and alternative splicing can be influenced by the speed of transcription [89]. It has been reported that splicing does not always progress sequentially from the 5' to the 3' end of a gene and with the same speed [90, 91]. Instead, different regions can be spliced rapidly or slowly [92]. A study of pig liver cells showed that for the *pCLEC4G* gene the first intron is spliced simultaneously with several more distal introns, while the second intron is spliced last [93].

Non-sequential intron removal can have unexpected consequences when mutations disrupt splice sites [94]. The splicing of the *COL1A1* gene region between exons 5 and 10 can follow two different routes. Removing introns 5, 6 and 9 is always rapid, while the excision of intron 8 can be before or after intron 7 [95]. Additionally, point mutations in splice signals were shown to cause skipping of exon 8, inclusion of intron 8 or inclusion of both introns 7 and 8. It is not clear yet which factors control the order of splicing. Theoretically, it might be influenced by the presence of intronic and exonic splice suppressors or enhancers, the "strength" of the donor and acceptor splice sites and/or the size of the intron [96, 97].

[1] https://github.com/pulyakhina/splicing_analysis_pipeline

[2] https://barmsijs.lumc.nl/HG/irina/example_data.tar.gz

Recursive splicing is another recently acknowledged feature of the splicing process. The principle of recursive splicing is that an intron might not be spliced in one piece. Instead, the spliceosome can recognize an intra-intronic sequence opposed to the canonical exon-intron border as a splice site, hereby removing the adjacent exon. The rest of such a partly spliced intron will be removed later, at once or again in multiple pieces following the strategy described above. Another type of multi-step intron removal [98] involves the usage of non-canonical donor and non-canonical acceptor splice sites. In this case an inner piece of intron is spliced first and a semi-stable lariat loop structure is formed and will be degraded later [99].

Alternative splicing cannot be fully understood when only mature mRNA is analyzed. When pre-mRNA molecules from different stages of splicing (pre-, intermediate- and post-splicing forms) are captured, the process of splicing can be studied in more detail and previously unknown splicing events can be identified. This type of analysis has been very challenging until recently. However, the development of high-throughput NGS, which involves highly parallelized sequencing of DNA or RNA, enabled the whole transcriptome analysis at high resolution [100, 101, 102]. In contrast to microarray analysis, RNA-Seq is a non-targeted approach, allowing the discovery of novel splicing events. Nevertheless, the analysis of RNA-Seq data is still a challenge, since NGS experiments generally produce millions of relatively short fragments (reads), even after paired-end sequencing came into play [103]. The distance between the two sequenced ends of a read pair ("PE distance") can be calculated and further taken into account during alignment. Standard mRNA analysis of (paired-end) RNA-Seq data includes mapping reads to the reference sequence, assembling the transcriptome and identifying the transcripts (transcript deconvolution), which is often followed by counting transcript levels (transcript quantification).

While mRNA analysis programs and pipelines are suitable for finding novel exons and exon-exon junctions, they do not consider the presence of pre-mRNA. Instead they analyze the end-result of the splicing process, using mainly reads mapped to exons. For this reason these tools are not able to properly deal with mixtures of pre- and mature mRNA, such as found in nuclear RNA extracts.

In this paper we are showing that splicing mechanisms can be analyzed using RNA-Seq data in more detail than previously achieved. We present *SplicePie* – a pipeline which contains new, dedicated method to analyze the order of splicing and pinpoint putative introns undergoing recursive splicing. Applying this method we show that non-sequentially spliced introns can be identified even in a relatively fast spliced gene. We also identify non-sequentially spliced introns in a gene that have never been reported to undergo such splicing scenarios.

2.3 Materials and methods

2.3.1 Captured dataset

Fused myotubes from a healthy human muscle cell line were harvested and the nuclei were separated from the cytoplasm using a sucrose containing lysis buffer, Dounce homogenizer and ultracentrifugation, respectively. Nuclear and total RNA were isolated from the nucleus using the Nucleospin RNAII column from BioKe Kit. DNAse treatment (RNAse-Free DNAse set by Qiagen) was performed to avoid DNA contamination. Three micrograms of each sample were reverse transcribed into cDNA (SuperScript II reverse transcriptase by Invitrogen), fragmented to the range of 100-600 bp by sonicating these samples with two cycles of one minute (Covaris S220, Massachusetts, USA) and purified (QIAquick PCR purification kit by Qiagen).

To capture target sequences we followed the SureSelect XT Target Enrichment System for the Illumina Paired-End Sequencing Library (Agilent Technologies). Illumina adapters were ligated to the fragmented sequences after end repair and A-base tailing (blunting). Further purification steps (performed with the Agencourt AMPure XP beads in 1:1 ratio) eliminated unbound adapters and short fragments (<100 bp).

The library of probes to capture exons, introns and flanking regions of the target genes (*FXR1*, *CKLF* and *ACTB*) was designed with the Agilent Technologies eArray software[3], avoiding areas masked by repeat masker and using partially overlapping probes. The 120 bp length probes were biotinylated four replicates of each probe were designed to reach the required number of baits per library.

The designed library [104] was hybridized with the fragmented cDNA from nuclear RNA and total RNA for 24 hours, followed by a washing step and pull down of the biotinylated cDNA probes using streptavidin- coated magnetic beads. Eluted samples were amplified to allow for a multiplexed Illumina run. The samples were quantified with the Agilent 2100 Bioanalyzer and Agilent HS DNA Chip Kit (Agilent Technologies, USA). The samples were diluted to a concentration of 7 pM and loaded onto an eight-channel flowcell and sequenced with the Illumina HiSeq 2000(Illumina, USA). After sequencing, *fastq* files containing paired-end reads (read length of 100 bp) and the base quality information were generated with CASAVA version 1.1 and used for further analysis.

2.3.2 ENCODE dataset

An RNA-Seq dataset representing a subset of the long RNA-Seq sequencing from ENCODE/Cold Spring Harbor Lab was obtained from the CSHL Long RNA-Seq downloadable files archive (Long RNA-Seq archive from ENCODE/Cold Spring Harbor Lab repository[4]. This dataset ("ENCODE dataset") contains RNA-Seq data from human immortalised myelogenous leukemia cell line, two samples of the chromatin-associated RNA and one sample of total nucleus RNA. These samples were sequenced by the Illumina Genome Analyzer II paired-end sequencing technique with read lengths of 75 and 100 bp.

2.3.3 General information

Alignment was performed with GSNAP version 2012-07-12 using a probabilistic mapping approach (one alignment per read was randomly chosen in case of multiple mappings). Format conversions were done with Samtools version 0.1.18 [39] and in-house scripts. Statistical manipulations and calculations were performed using R version 2.15.1. The Ensembl [105] gene annotation was used for all post-alignment analyses. Only publicly available software was used for the analysis.

2.3.4 Classification

After alignment, reads were classified according to their splicing stage. The first classification step determines the type of region that the reads are mapped to: exon, intron, exon-exon junction or exon-intron boundary (Table 2.1).

Each end of a read pair is given a label (Figure 2.1) and a "mapping distance". Mapping distance can be calculated for mapped read pairs by measuring the inner distance between the two aligned ends of a read pair.

Apart from classifying reads into three main categories, we divide them into more specific subgroups. Read pairs classified as intermediate-splicing reads are used for the analysis of sequentiality if one end is mapped to the exon-exon junction and the second end is mapped to the adjacent upstream or downstream intron. Read pairs having ends that are split across anything but an annotated exon-exon junction are used to identify recursive splicing (ends of a pair are treated separately and the connection

[3] http://earray.chem.agilent.com

[4] http://genome.ucsc.edu/cgi-bin/hgFileUi?db=hg19&g=wgEncodeCshlLongRnaSeq, file identifiers are:
wgEncodeCshlLongRnaSeqGm12878NucleolusTotal,
wgEncodeCshlLongRnaSeqK562ChromatinTotalRep3,
wgEncodeCshlLongRnaSeqK562ChromatinTotalRep4.

Table 2.1: Labels for reads based on the mapping location according to transcript annotation (j ¿ i).

Read start	Read end	Label
intron	intron	“int” (intronic)
exon$_i$	exon$_i$	“ex” (exonic)
exon$_i$	exon$_j$	“ex-ex” (exon-exon junction)
exon	intron	“ex-int” (exon-intron junction)

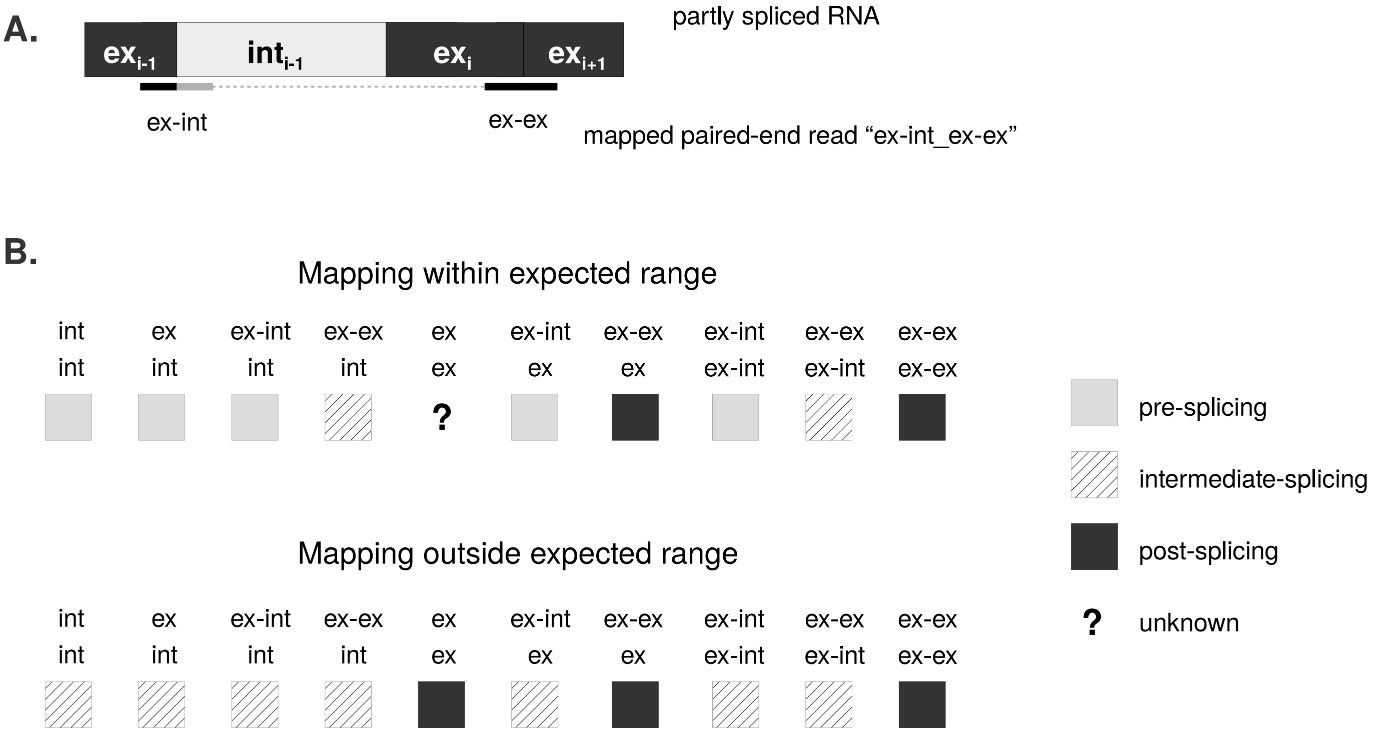

Figure 2.1: Classification of the paired end reads. **A.** “Mapping distance” reflects the inner distance between two read ends according to the genomic coordinates after alignment. **B.** Classification scheme is built on read labels (“ex” stands for exon, “int” for for intron, “ex-int” for intron-exon boundary, “ex-ex” for exon-exon junction) and mapping distance (within/outside expected mapping distance). Reads belonging to pre-, intermediate-, post-splicing and unknown categories are marked with gray, black, striped boxes and a question mark. Example: if one end of the read pair maps to the exon-intron boundary and the other one maps to the exon-exon junction, this read pair will be classified as “intermediate”.

between the ends is not considered). Ends of read pairs from the pre-splicing category mapped to the exon-intron boundary and read pairs from the post-splicing category (mapped to the exon-exon junctions) are used to calculate the Splice Site Index.

2.3.5 Detection of non-sequential splicing

Non-sequential splicing is approached from two angles: coverage-based and read-based approaches.

For the coverage-based approach the difference between the median coverage of intron$_{i+1}$ and intron$_i$ is reported (Figure 2.3). We select negative differences and define the cutoff of significance as the first quartile *Q1* (25% percentile). If the difference is bellow *Q1*, this is an indication that intron$_{i+1}$ is non-sequentially spliced before intron$_i$. This is calculated for every input sample. If a certain difference is consistent across a number of samples, the corresponding pair of introns is reported.

The read-based approach addresses read pairs that indicate whether two introns are spliced sequentially or non-sequentially (Figure S1).

For this we defined the *splice-ratio*, a value that reflects the fraction of reads supporting sequential splicing:

$$splice\text{–}ratio = \frac{seq}{seq + non\text{-}seq} \tag{2.1}$$

Here *non-seq* is the number of reads supporting non-sequential splicing and *seq* is the number of reads supporting sequential splicing of two adjacent introns. When introns are spliced sequentially, the splice-ratio will be close to 1. However, when a downstream intron is spliced before an upstream intron, the splice-ratio will be close to 0.

We improve the accuracy of the predictions by assessing how often independent read pairs support the same pair of introns being spliced sequentially. Single events might indicate false positives due to mapping artifacts (Figure 2.3).

2.3.6 Detecting recursive splicing

We hypothesize that if an intron undergoes recursive splicing, split reads will map across intermediate splicing products. Recurring observations of these specific products confirm the existence of partially spliced introns. To extract such reads, we first identify potential hotspots for recursive splicing (Figure S2). For each position we calculate how many times a read has been split over it (in other words, we calculated the "inverted coverage" – coverage of gaps) and then calculate the derivative of this inverted coverage. The derivative indicates where the inverted coverage changes relatively to the previous positions, implying how many reads share a breakpoint at that specific location. Positive values represent a split's start, while negative values indicate a split's end. All other positions will have a derivative value of zero. Each peak is reported in a *wiggle* file. Positions which are start- and endpoints for splits at the same time are excluded from this analysis. Reads spanning exon-exon junctions are also removed, as they indicate annotated exon-exon junctions and do not contribute to the investigation of recursive splicing.

In order to reduce the amount of noise and false positives, we create *wiggle* files for all input samples and evaluate the overlap in the requested number of samples. If the position has positive coverage in a number of samples, the sum of the coverage from all files will be reported. This results in a single file with the most robust positions. Reads covering the positions from the final list are extracted from the initial *bam* file(s) and analyzed to validate the prediction of recursive splicing hot spots from the *wiggle* file and get the connections between the peaks (which are lost in the *wiggle* file).

Additionally, a text file containing a matrix with all discovered junctions and the number of reads supporting each junction is created per gene (Figure 2.4).

2.3.7 Calculating Splice Site Index and processing the coverage

We developed the Splice Site Index (SSI), a value used to detect splicing events, which is calculated in the following way:

$$SSI = \frac{ex\text{-}ex}{ex\text{-}ex + ex\text{-}int} \tag{2.2}$$

Here *SSI* is the splicing index value, *ex-ex* is the number of reads spanning exon-exon junctions and *ex-int* is the number of reads spanning exon-intron junctions.

A similar function, called completed Splicing Index (coSI), has been recently developed [6]. In contrast to coSI, SSI is calculated separately for 5' and 3' splice sites of each intron, allowing for the assessment of a) the relative abundance of each intron and b) whether both ends are spliced simultaneously. SSI, in combination with the median coverage of introns and exons, gives a more complete picture of the alternative splicing events. SSI is calculated as a ratio of different types of reads and does not consider the difference between the absolute values of coverage.

2.3.8 Experimental validation of non-sequential and recursive splicing

Complementary DNA (cDNA) from three different healthy muscle cell lines (also used in the *in silico* analysis) was generated using the reverse transcriptase, 1 μg of pre-mRNA and random primers (following the standard protocol suggested by SuperScript III RT by Invitrogen).

For the validation of non-sequential splicing, forward primers were designed against exon 10 or intron 11. Reverse primers were designed against exon 11 or the junction of exon 11 and exon 12. All combinations of primers were used to detect all splicing intermediates that can be formed in this area of the gene. Each sample was analyzed with three technical replicates and normalized against the *HPRT* gene. QPCR was performed on the LightCycler 480 (Roche Diagnostics Ltd.) using SYBR Green mix. QPCR results were analyzed using LightCycler 480 and LinRegPCR software [106]. Independent amplification, with primers in intron 10 and exon 12, was performed for further Sanger sequencing analysis.

For the validation of recursive splicing events, we amplified the same synthesized cDNA template using a pair of primers located upstream of the predicted donor and downstream of the predicted acceptor splice sites. For the event with one non-annotated splice site the forward primer was located in exon 16 and the reverse primer was located in intron 16. For the event with both non-annotated splice sites both primers were located in intron 16. PCRs were performed with 35 cycles using Phusion High-Fidelity PCR 2X Master Mix with HF Buffer (New England BioLabs Inc).

The amplification products were then separated on a 1.5% agarose gel after an RT-PCR reaction. The dissected bands were extracted and eluted (MinElute gel extraction kit, Qiagen) and sequenced with Sanger sequencing.

2.4 Results

2.4.1 Pipeline overview

SplicePie starts with a standard quality check procedure, removes low quality reads and performs split read alignment to the reference genome. The gene of interest is then extracted from the alignment file and is used to calculate the Splice Site Index (SSI) and classify reads based on their stage of splicing (pre-, intermediate- and post-splicing, see Section 2.3.4 and Table 2.1 for details). Reads from specific categories are used to predict and pinpoint putative non-sequentially or recursively splice introns. An overview of *SplicePie* is shown in Figure 2.2.

Alignment to the reference genome (hg19, GRCh37) is performed using GSNAP [107], an aligner that works with paired-end RNA-Seq data and can split each read end into multiple fragments, thereby coping effectively with a gene's intron/exon structure. We have chosen GSNAP over Tophat [62, 108], PASSion [36], HMMSplicer [109] and MapSplice [96] because, unlike these tools, GSNAP does not give priority to split alignments. This is crucial for pre-mRNA data, as such data contains reads across exon-intron boundaries. Unlike other tools, GSNAP uses the information about canonical and non-canonical splice sites when splitting the reads, which is important for the identification of novel exons. It is also able to split each read of the pair into as many fragments as necessary (in case of multiple adjacent small exons). GSNAP provides the results in the commonly used *sam* format. *SplicePie* generates *bam* and *wiggle* files from these *sam* files. Our analysis approach is mostly suitable for very detailed analysis, therefore it is recommended to analyze one gene of interest at a time.

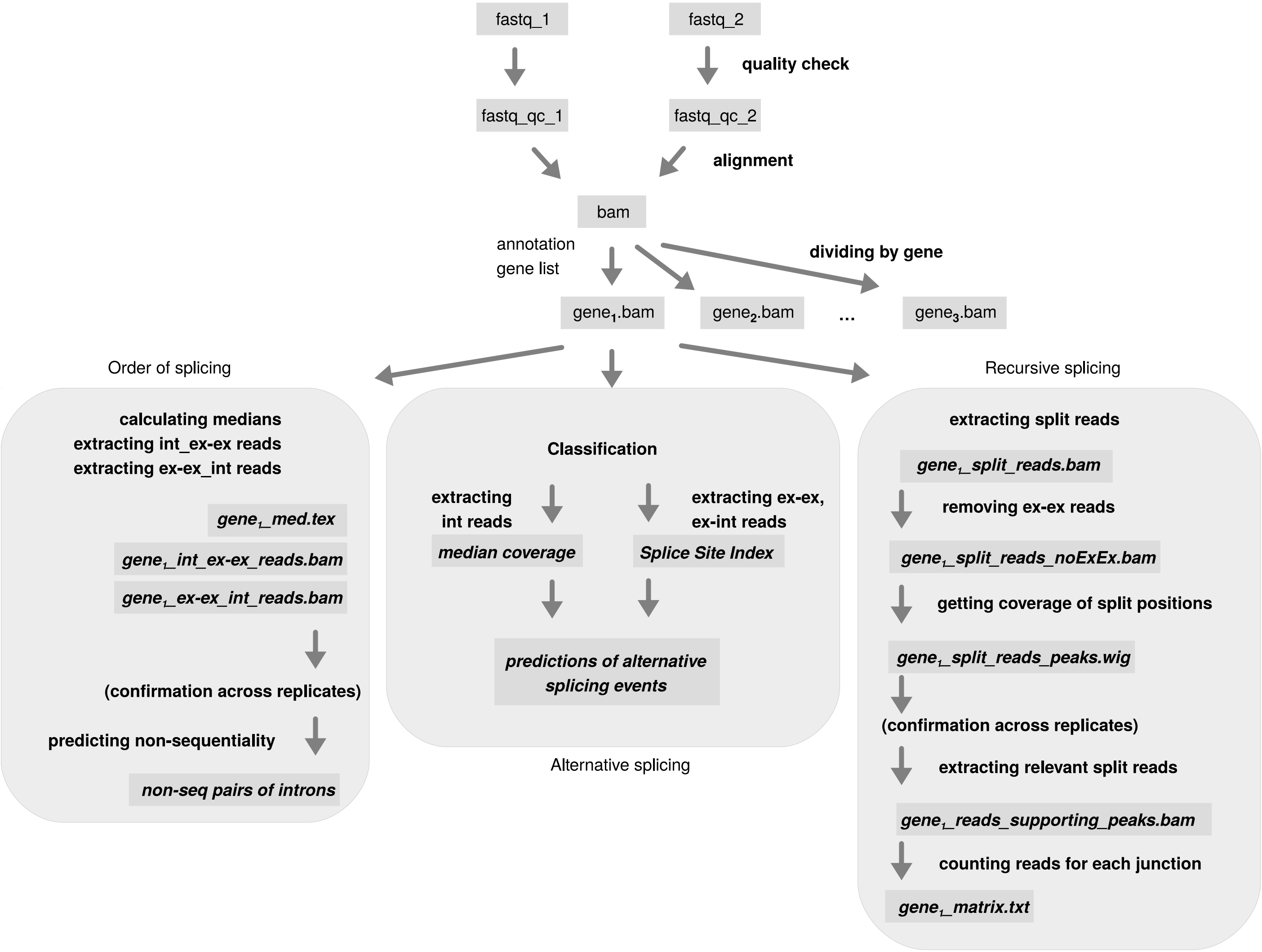

Figure 2.2: Lay-out of *SplicePie*. Light-grey boxes indicate the files required/produced during the mainstream analysis. Labels in **bold** next to the arrows indicate the steps of analysis. Labels in *italic* next to the arrows indicate the additional input files. Label *int_ex-ex* indicates that the file contains read pairs with one end mapped to the intron and the other end mapped to the exon-exon junction (and vice versa for *ex-ex_int*).

However, running *SplicePie* for multiple genes is also supported and all gene annotations provided by the user in a standard *GTF* format will be used to build a list of the genes of interest. *SplicePie* performs the classification of reads as pre-, intermediate- or post-splicing according to their mapping position (see Section 2.3.4 for details). After classification all reads spanning a specific exon-exon junction or an exon-intron boundary are used for the SSI calculation. SSIs will then be calculated for each splice site (see Section 2.3.7 for details). The output is provided as a *text* file containing SSIs for both 5' (SSI^5) and 3' (SSI^3) ends per intron. SSI value is calculated using the reads spanning exon-exon junctions and exon-intron boundaries. This value is similar to the completed splicing index, *coSI* [6], which reflects the amount of RNA molecules containing the exon with spliced adjacent introns. However, SSI is calculated separately per splice site and therefore reflects the difference between 5' and 3', thereby highlighting alternative splicing and/or incomplete splicing (while *coSI* reflects the completion of the splicing of a particular intron).

A parallel branch of *SplicePie* is analyzing the order of splicing and predicts which introns are spliced sequentially and which introns are spliced non-sequentially. Median coverage of each intron is calculated and when the difference between the downstream intron_{i+1} and the upstream intron_i is low, such pair of introns is potentially non-sequentialy spliced. At the moment we define this value as "low" when it is below *Q1*, where *Q1*, or lower quartile, is defined as the middle number between the smallest number and the median of the dataset (Figure 2.3, A).

Another branch of *SplicePie* processes the *wiggle* files and pinpoints introns potentially undergoing recursive splicing. The *wiggle* files contain only the coverage of splice sites. We take all combinations of donors and acceptors and calculate the number of reads supporting them. This creates a summary matrix containing all potential recursive splicing events and their frequency in each sample (Figure 2.4).

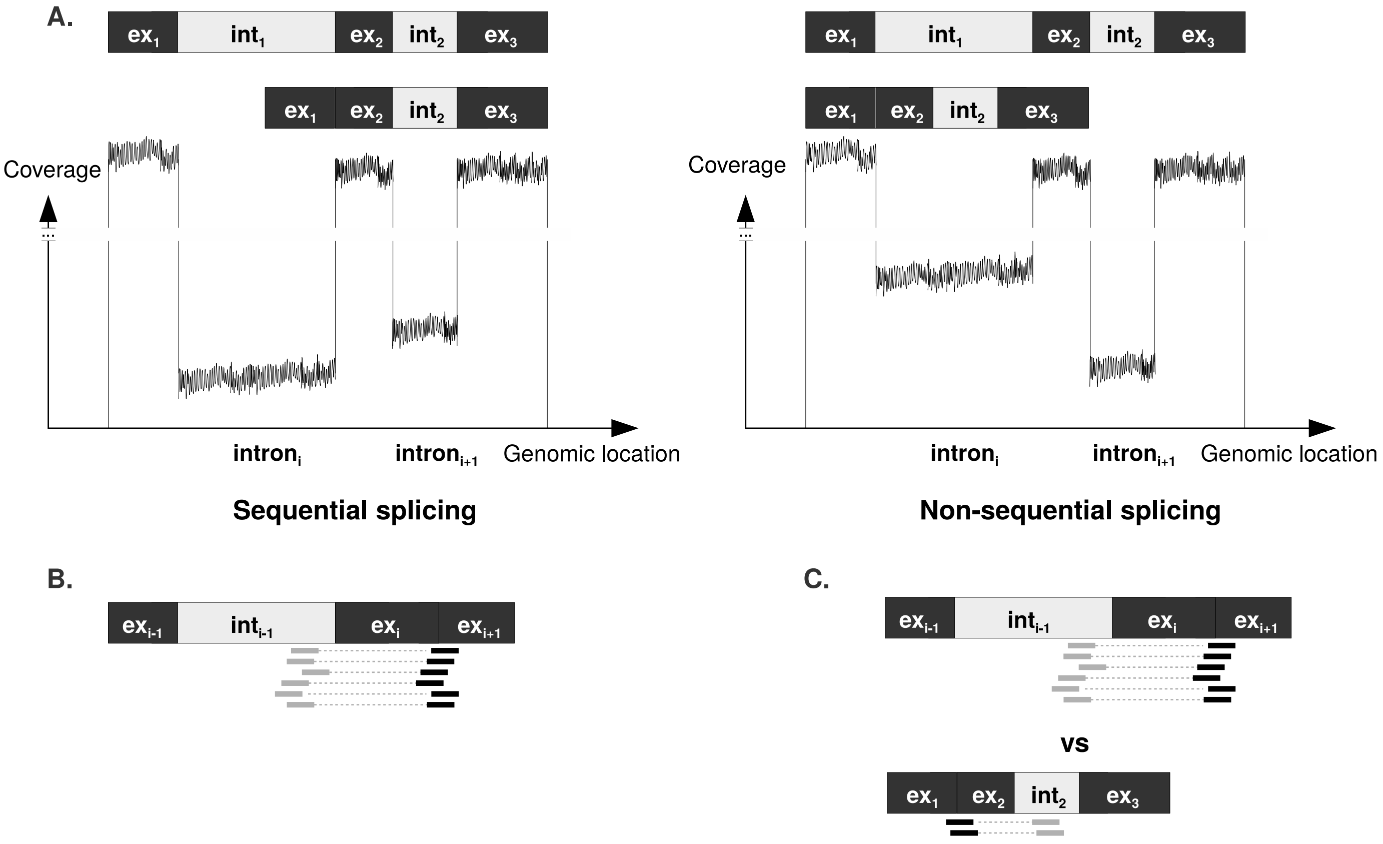

Figure 2.3: Principles of the two approaches to investigate non-sequential splicing. **A.** Coverage-based approach with the underlying assumption that the longer the intron is present in the sample, the higher the coverage will be. In case of non-sequential splicing the coverage of the downstream intron$_{i+1}$ is likely to be lower than the coverage of the upstream intron$_i$. Median of the coverage of each intron is used in this approach. **B.** The underlying assumptions for the read-based approach to detect non-sequential splicing: evidence for non-sequential splicing is obtained from read pairs with one end mapped to the upstream intron$_i$ and the other end mapped to the junction over the downstream intron$_{i+1}$ (exon$_{i+1}$-exon$_{i+2}$ junction). **C.** Method to select the introns with non-sequential splicing. The read pairs supporting the splicing intermediate where intron$_i$ is spliced before intron$_{i+1}$ should be less abundant than the read pairs for the intermediate product where intron$_{i+1}$ is spliced before intron$_i$.

2.4.2 Alternative splicing events in captured dataset

Four nuclear RNA, four total RNA and one DNA sample (Table S1) were sequenced (see Section 2.3.1 for details). The analysis of the target gene – *FXR1* – will be discussed in this section. From the targeted genes, we have studied the pre-mRNA splicing of (70,306 nt long) in detail because it is known to be alternatively spliced, has an intermediate number of exons (18), introns with variable length between 86 and 18,338 nt and a decent intronic coverage (on average above 1,500 for nuclear RNA samples) in the cell lines analyzed (Table S1). Note that the numbers of reads for the categories do not always add up to the total number of reads mapped to the target, since we do not show the number of reads defined as 'unclassified' (see Section 2.3). The classification of reads into three categories supporting pre-, intermediate- and post-splicing events is used to estimate the pre-mRNA content of samples (see Section 2.3.1 for details). Compared to the total RNA samples, all nuclear RNA samples contain a larger fraction of reads coming from the pre-splicing stage (Figure 2.5). This is expected, as total RNA is isolated from the whole cell and consists mostly of mature messenger RNA, while nuclear RNA contains (partly) spliced RNA. The post-splicing category contains a large fraction of reads even in nuclear RNA samples, which might be a consequence of the fast splicing of *FXR1*, which makes it hard to capture the nuclear pre-mRNA of this gene. Reads from the DNA sample were mainly classified as “pre-splicing”, which is expected, since DNA is not supposed to contain any exon-exon junctions.

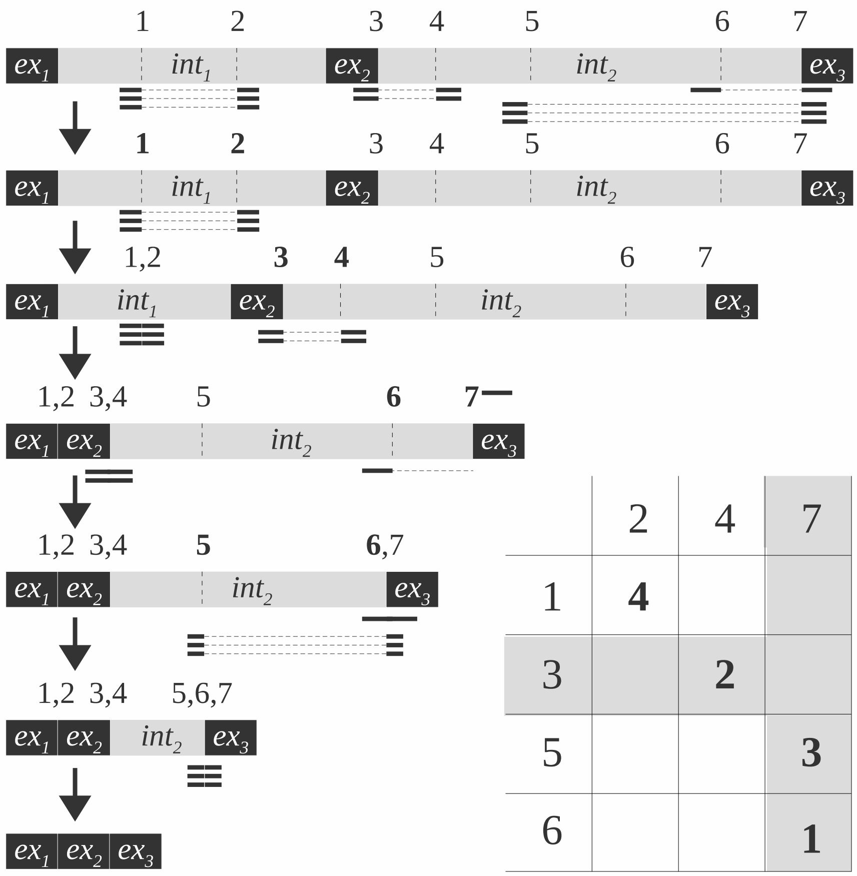

	2	4	7
1	**4**		
3		**2**	
5			**3**
6			**1**

Figure 2.4: Graphical representation of the analysis of recursive splicing. Black boxes represent exons and grey boxes represent introns, dashed lines across the introns and exon-intron borders represent positions of splits in reads. Numbers “1”, “2”, etc. on top of the gene schema represent the positions of the gene in genomic coordinates. Thick lines connected with dashed lines represent split reads (where the dashed part of the line represents the area across which the read is split). Step-by-step analysis of all split reads is shown and splicing intermediates corresponding to each group of split reads are shown on the schema in left part of the figure. The matrix in the right bottom corner contains donor splice sites (top row) and acceptor splice sites (left column). Each cell in the matrix represents the number of reads supporting such junction. Numbers in the gray cells of the matrix represent reads with one new non-canonical splice site. Numbers in white cells of the matrix represent reads with two new non-canonical splice sites (reads split within an intron).

In order to investigate alternative splicing events we use a combination of SSI values and medians of intronic and exonic coverage.

As the coverage may be influenced by the probe hybridization efficiency, we evaluated the uniformity of the coverage in the DNA sample D1 (Figure S3). The only dips in coverage take place in the Repeat Masker regions, which were excluded from probe design (Figure S4). To confirm the limited influence of probe hybridization on coverage, we calculated the standard deviation of the median coverage per intron, which was only 11.52% of the average.

Median coverage has been calculated per intron, while SSI is calculated per 5’ and 3’ end of each intron separately. SSI can indicate various alternative splicing events, i.e., (partial) intron retention and exon skipping (data shown for sample N2, Figure 2.6).

Decreases in the SSI^5 of intron 2 and in the SSI^3 of intron 1 are indicative of the skipping of exon 2 in a subset of transcripts. This is confirmed by the relatively low coverage of exon 2. The coverage of

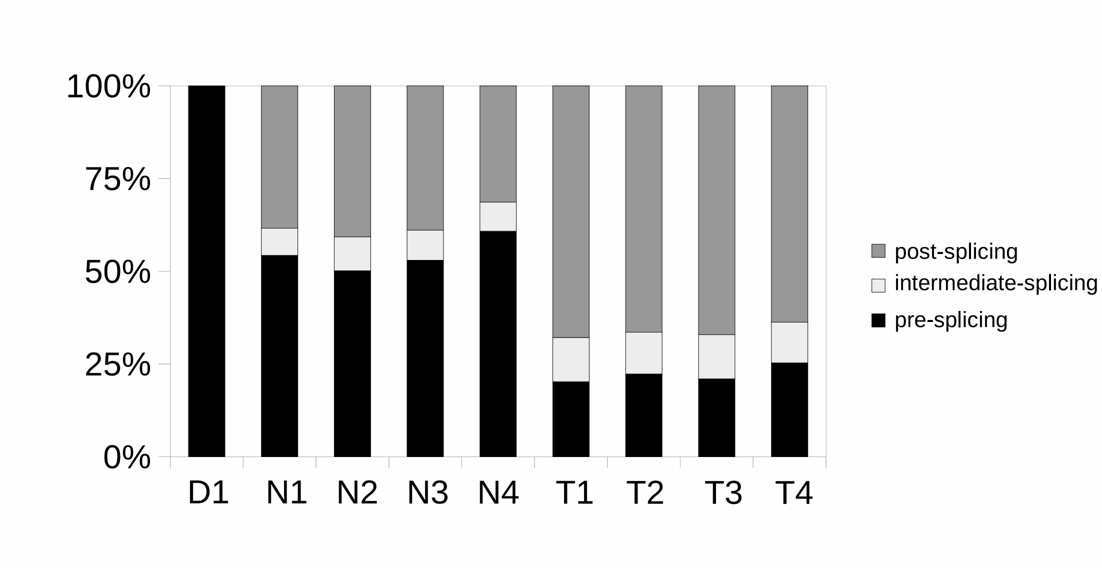

Figure 2.5: Classification of reads from the capture dataset mapped to *FXR1*. For sample identifiers see Table S1. The figure displays the percentage of reads mapped to *FXR1* classified into pre-, intermediate- and post-splicing fractions for pre-mRNA and total RNA samples in the captured dataset.

intron 13 is significantly higher than the average intronic coverage, which can indicate intron retention in both pre- and mature mRNA. This is also supported by low SSI^5 and SSI^3 values of intron 13, which means that the number of reads mapped to the boundary of exon 13 and intron 13 and the boundary of intron 13 and exon 14 are overrepresented. The retention of intron 13 and skipping of exon 2 were experimentally confirmed for sample N2 (Figure S5). Thus, low SSI^5 and SSI^3 on the same intron are the indication of an intron retention, whereas low SSI^3 of an intron in combination with low SSI^5 of the next intron is an indicator of exon skipping.

We also developed a module to rank introns based on their probability to be retained. For retained introns, both SSI^5 and SSI^3 values should be low. To estimate that, we calculate the magnitude of SSIs (how big the difference between SSI^5 and SSI^3 values is) and the likelihood of each magnitude (Appendix). The introns with the highest magnitude and a low p-value are the main candidates for retention (Table S2).

2.4.3 Non-sequential splicing in captured dataset

In the captured dataset, we searched for non-sequentially spliced introns in *FXR1*. Multiple candidate pairs of introns with a difference in median coverage below *Q3* were found: introns 1 and 2; introns 3 and 4; introns 10 and 11; introns 16 and 17. (Here Q3 stands for the third quartile – the middle value between the median and the highest value of the data.) To confirm this, we calculated the ratio of read pairs in support over those not in support of non-sequential splicing. If the splice-ratio is close to *1*, the splicing is most likely sequential, the lower the ratio is, the more non-sequential splicing occurs. We observed a very strong correlation between both methods, supporting the idea that these methods are suitable to identify non-sequentiality spliced introns (Pearson $R^2 \leq 0.86$ and Spearman $R^2 \leq 0.85$ (Figure S7).

We used DNA as a negative control, since DNA does not undergo splicing and the coverage of the introns should not differ significantly. If introns have significantly different coverage on DNA level, this may be due to sequencability, mappability bias or other technical artifacts (not a biological reason). Two pairs of introns predicted to undergo non-sequential splicing in RNA samples (introns 3 and 4; introns 10 and 11) survived this extra control step. They were not classified as non-sequentially spliced in DNA. Introns 10 and 11 have been selected for further the experimental validation and showed to be non-sequentially spliced (Figure 2.7).

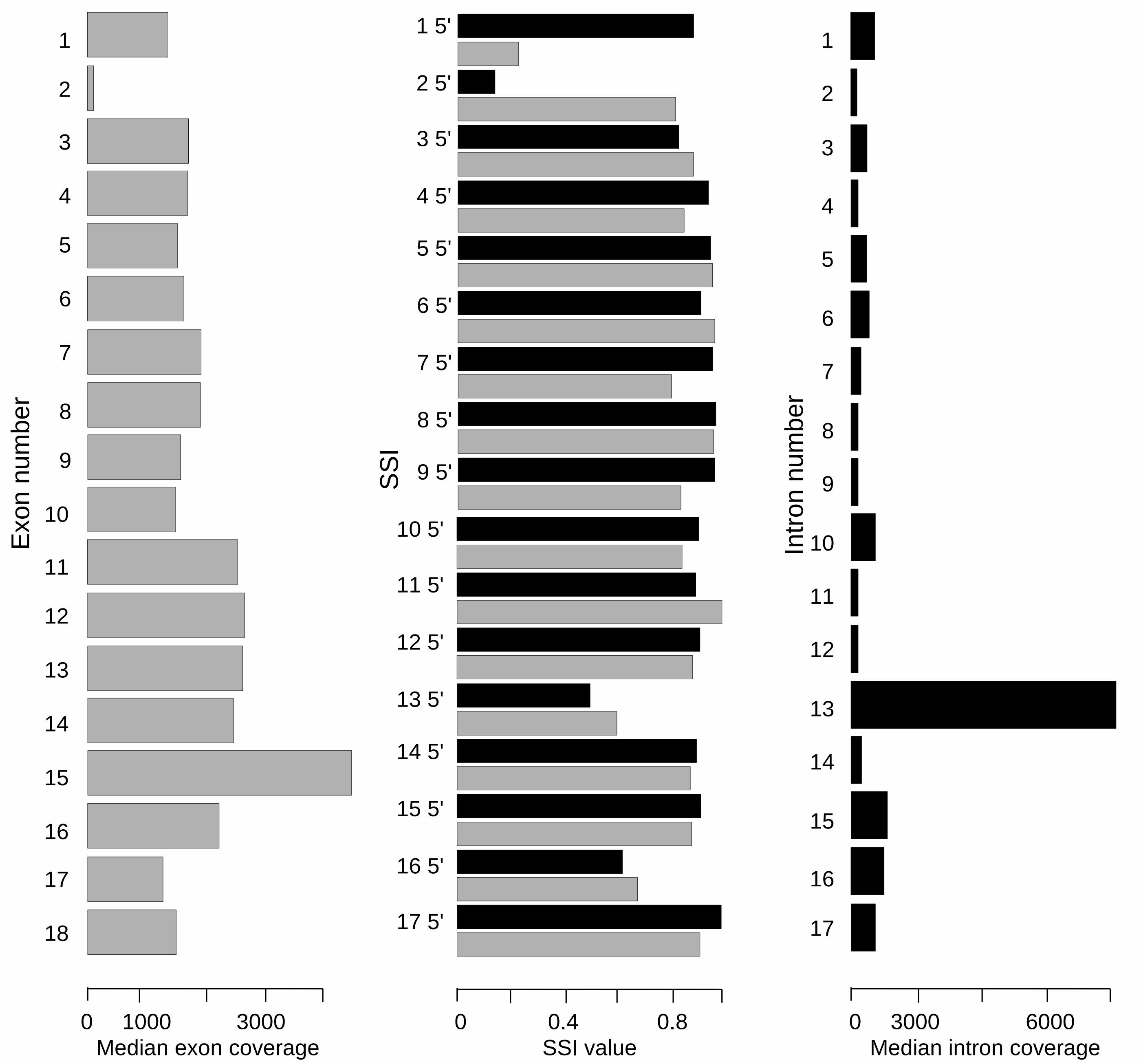

Figure 2.6: Splice Site Index (SSI) and medians of coverage of exons and introns in *FXR1*. Gray bars in the left panel represent the coverage of exons (exon 1 on top). Black bars in the middle panel represent SSI^5 values the introns and gray bars on the middle plot represent SSI^3 values of the introns (intron 1 on top). Black bars in the right plot represent the coverage of introns (intron 1 on top). Data shown for nuclear RNA sample N2.

2.4.4 Recursive splicing in captured dataset

We searched for the evidence of multi-step splicing in our captured dataset (as described in Section 2.3.6). *Wiggle* files containing coverage at positions where the reads were split have been created for four pre-mRNA samples (reads spanning exon-exon junctions were excluded). We considered positions present in all samples with the same sign for further analysis, because they were deemed most reliable.

We assessed the distribution of peak coverage and tried to identify the minimal coverage for the peak to be included in the final list. We first investigated the highest peaks and found out that the coverage of the regions between the peaks is higher compared to the rest of the introns. These observations let us hypothesize that such intronic regions with high coverage and split reads mapped to them and to the

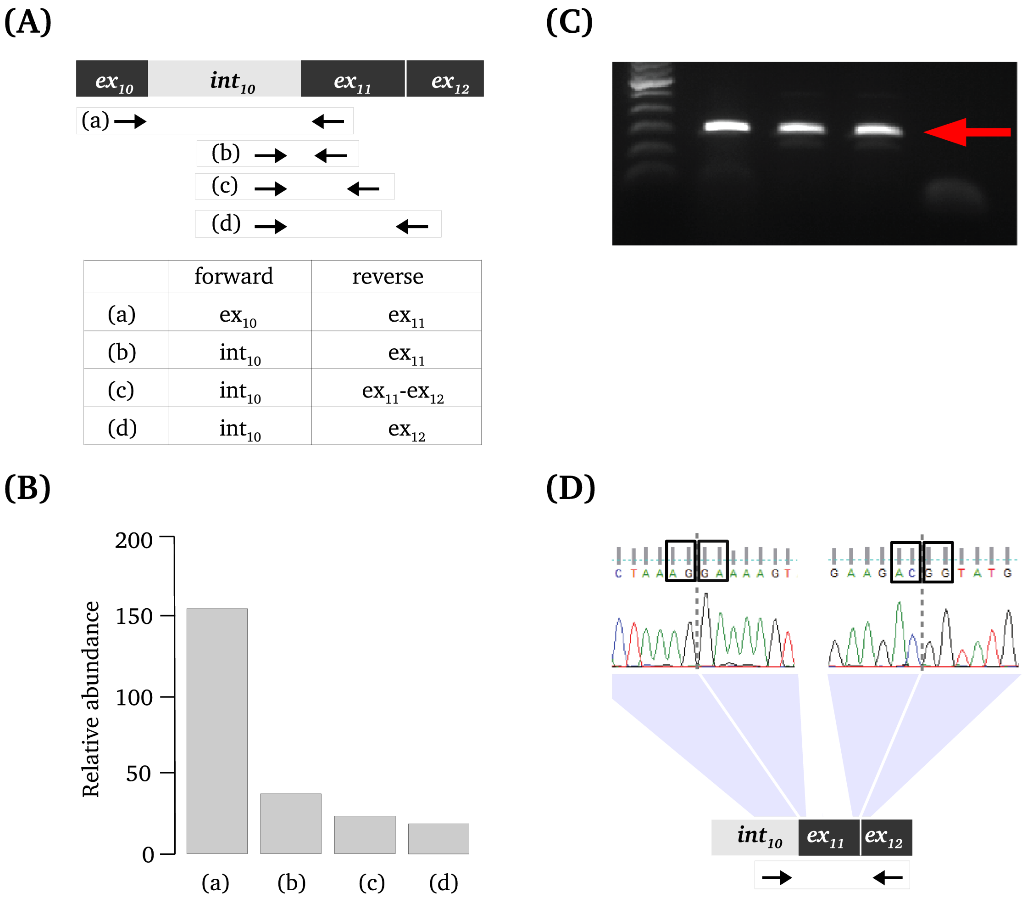

	forward	reverse
(a)	ex_{10}	ex_{11}
(b)	int_{10}	ex_{11}
(c)	int_{10}	ex_{11}-ex_{12}
(d)	int_{10}	ex_{12}

Figure 2.7: Experimental validation of predicted non-sequential splicing of introns 10 and 11 in *FXR1*. **A.** The design of the primers for the validation of non-sequential splicing of intron 10. **B.** The results of quantitative real-time PCR showing the relative abundance (on the Y axis) of splicing intermediates with primer combinations described in **A** (on the X axis). Since three tested cell lines showed similar reproducible results, the figure shows the average. **C.** Results of PCR showing the presence of the fragment of anticipated size. Lane 1 contains the marker, lanes 2, 3 and 4 represent three cell lines, lane 5 shows the negative PCR control. **D.** The results of Sanger sequencing of the band shown on **C**. The top panel shows the output of Sanger sequencing, black box around “AG” depicts the acceptor splice site, the boxes around “GA”, “AC” and “GG” depict ends of the exons. The bottom panel shows the design of the primers for the sequenced amplicon.

adjacent exons might be novel exons. We were able to experimentally validate one of potential novel exons (Figure S6). Our findings thus suggest that the method developed for the detection of recursive splicing events is also suitable for finding novel exons.

After excluding the peaks with the highest coverage we found eight events to be recurrent and consistent across all RNA samples (Table S3). These events were not present in the DNA sample D1, which had only 61 split reads (against hundreds of split reads in RNA samples), none of the split positions was supported by more than one read. The vast majority of split reads in DNA were mapped with a large number of mismatches (unlike split reads in RNA samples).

The most abundant events of recursive splicing occurred on the 5’ end of the intron (when the donor splice site is canonical and the acceptor splice site is situated within the downstream intron, Figure S8). The second biggest class (three cases, or around 40%) were the cases of recursive splicing occurring on the 3’ end of the intron. We also found a pair of events with shared canonical acceptor splice site (the intron 10-exon 11 boundary), which suggests the possibility of multi-step recursive splicing in this area (Figure S9). Furthermore, we were also able to identify one recurrent event of inner recursive splicing with two non-canonical splice sites (Figure S10).

The strength of the newly identified donor or acceptor splice sites associated with potential recursive splicing events was assessed with Human Splicing Finder[5]. All sites were identified as highly probable putative splice sites.

To obtain further evidence that the recursive splicing events identified by *SplicePie* are genuine, we evaluated the sequence motifs flanking the splits. We selected events present in two, three, four or five out of five samples and extracted the splice sites and two nucleotides upstream of the donor and

[5] http://www.umd.be/HSF3/HSF.html

downstream of the acceptor sites. We calculated the percentage of canonical and non-canonical donor and acceptor splice sites in the events with non-annotated donor or acceptor splice site. In this analysis we omit potential recursive splicing events with both non-annotated splice sites, as they are more likely to be novel exons. Such events require further experimental validation, and only experimentally showing there presence in pre- and possibly mature mRNA will distinguish between recursive splicing and novel exons.

Our results (Table S4) show strong enrichment for canonical donor (GT) and acceptor (AG) splice sites for events with one non-annotated splice site present in five samples. The enrichment becomes weaker for the events detected in only a subset of the samples, especially for the events with a non-annotated acceptor site. This indicates that the recurrent events with one non-annotated splice site are the most robust recursive splicing events. Note that the aligner we use does not have any preferences for splice motifs when splitting reads.

Apart from the *in silico* validation, we also used RT-PCR followed by Sanger sequencing to validate potential recursive splicing events. We designed primers flanking two events found in all five samples and analyzed nuclear and cytoplasmic RNA isolated from two of the muscle cell lines. For the first event, (chr3:180,689,975-180,692,201, Table S3), detected a product of the expected length and sequence. However, it was found in both nuclear and cytoplasmic RNA, suggesting that the detected event represents a novel exon and not an intermediate splicing product. The second set of primers captured another recursive splicing event that was not present in the RNA-Seq data.

2.4.5 Performance on non-targeted dataset

To demonstrate the performance of *SplicePie* on regular, non-targeted RNA-Seq data, three samples from the Gencode project (the ENCODE dataset) containing RNA from different nuclear compartments (chromatin- associated and nucleolus RNA) were analyzed following the same procedure as the captured dataset. Around 95% of reads mapping to the *FXR1* gene were classified as pre-splicing for chromatin and nucleolus RNA in contrast with 20 and 60% for the nuclear and total RNA samples, respectively. This is in line with the presence of pre-mRNA in chromatin and nucleolus, while mature mRNA is prevailing in the nucleoplasm.

The values of SSI and medians of exonic and intronic coverage for the non-targeted RNA dataset (Figure S11) coincide with corresponding values calculated for the captured dataset. Low SSI^3 for intron 1 and low SSI^5 for intron 2 indicate the skipping of exon 2 and high coverage of intron 13 together with its low SSI^5 and SSI^3 are indicative of intron 13 retention. However, the pattern of the medians is less consistent for both exonic and intronic coverage. The C1 sample contains chromatin-associated RNA, for which splicing is not known to be in action, the difference between the exonic and intronic coverage is small, therefore the coverage values for chromatin-associated RNA are less informative than those for nucleoplasmic RNA.

We were able to confirm the previous findings (of intron 10 and intron 11 being non-sequentially spliced) using the approach based on median intron coverage (see Section 2.3.5 for details). Other predictions were mostly confirmed in at least two out of three analyzed samples with the coverage-based approach (data not shown). However, the number of reads needed to calculate the splice-ratio was not high enough, so the majority of the ratios equalled zero.

The non-targeted RNA dataset was also analyzed in order to find potential recursive splicing events. Five peaks were present in all three samples. Two of these peaks were found in the list of donor/acceptor splice sites identified for the captured dataset. The number of splice sites identified per sample was approximately 100, while the number of peaks for each sample of the captured dataset was over 450.

In order to demonstrate the performance of *SplicePie* on the whole-transcriptome dataset, we selected *TIA1* for the analysis of non-sequential and recursive splicing.

Based on the difference in median intronic coverage (which was at least three times higher than the upper quartile (75%) in all three samples) and high splice-ratio (average of 0.7 in the three samples), we could predict two introns of *TIA1* to be non-sequentially spliced. Neither intron 2, nor intron 3 are overlapping with any genomic elements that might influence the coverage, such as pseudogenes or non-coding RNAs.

According to both considerable difference in coverage and high splice-ratio, intron 3 is predicted to be spliced before intron 2 (Figure S12). Even more cases of potential non-sequential splicing were found in two out of three samples, however, to claim that the order of splicing of these introns is non-sequential, experimental follow-up is required.

We also investigated multi-step splicing in *TIA1* and were able to detect a number of potential recursive splicing events. Events present in all three samples C1, C2 and U1 with non-annotated donor, non-annotated acceptor and both non-annotated splice sites were detected (Table S5).

Therefore, non-targeted total RNA-Seq data provides sufficient information to analyze recursive splicing for some genes and can be used for the detailed investigation of splicing in action.

2.5 Discussion

Exploring pre-mRNA processing is facilitated by new sequencing technologies reaching higher throughput, hence producing more data. The analysis of both pre- and mature mRNA provides new insights into splicing mechanisms and alternative splicing events. However, current software is focusing on mature mRNA and the identification (and quantification) of transcript variants.

The presented pipeline for the pre-mRNA data analysis, *SplicePie*, offers a number of approaches and solutions to study splicing in more details. The proposed strategy performs well on different sample preparations (sequencing the whole pool of RNAs, or capturing a gene with different relative quantities of pre- and mature mRNA). Our method can detect various genuine alternative splicing events like intron retention, exon skipping and novel exons. Furthermore, it is capable to resolve the order of splicing and recursive splicing events.

The methodology of *SplicePie* significantly differs from existing pipelines, such as Cufflinks, Scripture [110] or MISO [111]. These tools focus their analysis on the end result of splicing and mainly use reads mapped to the exons or exon-exon junctions. Reads mapped to the introns are either treated as putative exons or not addressed at all (in case of annotation-based pipelines). Therefore these pipelines are not able to analyze mixtures of pre- and mature mRNA (as found in nuclear RNA extracts). This is crucial to understand the details of the splicing mechanism. Our pipeline *SplicePie* is specifically geared towards the analysis of the full splicing process in action. In order to do so, it uses all reads mapped to exons, introns, exon-exon junctions or exon-introns boundaries.

For the analysis of alternative splicing events, the SSI and the medians of exonic or intronic coverage methods implemented in *SplicePie* are mutually reinforcing. In case of captured data enriched with partly spliced nuclear RNA, the difference in exonic and intronic coverage makes the patterns of coverage informative for assessing alternative splicing events. In case of "pure" nuclear RNA with lower abundance of spliced fragments, the difference in exonic vs. intronic coverage drops, however, the SSI values become more informative.

The main novelty of the methodology introduced in this paper is the possibility to analyze splicing order and the stepwise nature of splicing. While we are able to judge local splicing order, i.e. one intron is spliced before a neighboring intron, it is not possible to determine the global order of splicing for the entire transcript. This happens due to the co-transcriptional nature of the splicing process and the fact that we capture only one snapshot of the nascent transcript. We show that the local order of splicing for certain introns within *FXR1* is reproducible (in biological replicates) and even consistent across multiple cell lines. Furthermore, this can be confirmed with independent PCR-based technologies.

Although the fact that splicing can be performed in multiple steps has been known for over a decade [112], however, it has never been analyzed bioinformatically. We show that analyzing the intermediate category of reads is possible for both potential novel exons and recursive splicing events. However, focusing on a narrow fraction of reads might result in analyzing random events, which is why we suggest to use as many samples as possible. To improve reliability even further it is advised to select events occurring in a significant number of samples. This strategy also helps reducing biases introduced by PCR duplicates, which are not likely to appear at the same position in replicates. The splice motif analysis of potential recursive splicing events provides evidence that these events are genuine, considering the canonical splice motifs and the occurrence of the events across multiple cell lines. However, as RNA-Seq is more sensitive than PCR, not all detected events can be experimentally confirmed at the moment. Recursive splicing events with both non-canonical splice sites should be treated especially carefully, as for these events it is hard to distinguish between recursive splicing and novel exons without the experimental validation in both nuclear and cytoplasmic RNA.

Detecting background noise is a common problem in bioinformatics and statistics, especially when working with large datasets containing a mix of introns and exons. Our approach was shown to perform well on both high (captured dataset) and low (non-targeted ENCODE dataset) coverage data. Moreover, despite the combination of low coverage and noise, alternative splicing events were detected reliably. This indicates that total RNA sequencing can be used for detecting non-sequential splicing events relying mainly on coverage information. *SplicePie* can be run on any dataset and the main concern is the average coverage of the introns. Even recent total RNA sequencing protocols do not provide enough intronic coverage to perform the analyses as powerful and reliable as the analyses on captured data. Our study shows that even total RNA sequencing of specifically nucleus does not generate enough coverage to detect non-sequential and multi-step splicing as efficiently as captured RNA libraries. Due to low intronic coverage total RNA can be used to analyze splicing and certain events will be detected, however, a lot of events will be missed. Therefore, we would still recommend to do the targeted sequencing of the genes of interest to allow a more in depth analysis.

Using *SplicePie* on different datasets revealed various not yet annotated splicing events. Our work enhances the value of pre-mRNA sequencing data and pioneers the investigation of the mechanisms of (alternative) splicing.

2.6 Acknowledgements

We thank M. van Iterson and S.P. van Leeuwen for their help with statistical analysis, M. Vermaat for his help with software development, M.P. Villerius for the help with running the analysis of the cluster, M. van Galen for his extensive help with this manuscript and W. Arindrarto for suggesting the name of the pipeline. This work was funded by ZonMW (project code NWO VIDI 91710303 to AAR) and by the European Commission 7th Framework Program, Project N. 261123 (GEUVADIS).

2.7 Appendix

Table S1: Characteristics of samples and summary of results for reads mapped to *FXR1*. For each sample the reads were classified as pre-, intermediate- or post-splicing based on the distance between paired ends (<650 being normal and >650 being larger than anticipated). Samples D1-T4 are from the captured dataset, samples C1-U1 from the ENCODE dataset.

sample	description	reads	norm.	norm.	norm.	large	large
name		mapped	pre-spl.	int.-spl.	post-spl.	int.-spl.	post-spl.
		on target					
D1	DNA	306103	286501	148	29	209	6
N1	**n**uclear RNA1	317827	139084	11834	64750	6879	33688
N2	**n**uclear RNA2	586827	224231	28520	134229	12336	47954
N3	**n**uclear RNA3	431321	184823	15845	91217	12456	44680
N4	**n**uclear RNA4	1394314	707109	51856	222918	39003	141707
T1	**t**otal RNA1	242979	41232	11347	81826	9456	41048
T2	**t**otal RNA2	181383	28002	9234	62588	7222	31376
T3	**t**otal RNA3	261004	42412	10932	67126	13111	68536
T4	**t**otal RNA4	317123	60915	12528	81132	13901	72375
C1	**c**hromatin RNA1	21632	19445	169	489	77	209
C2	**c**hromatin RNA3	8600	7251	62	189	39	91
U1	n**u**cleolic RNA	20283	16566	173	152	123	158

Table S2: Predicting intron retention events based on the magnitude of the SSIs and the *p*-value. Column "$5'$ ex-int" contains number of reads mapped to the exon-intron boundary on the 5'-end of an intron (used to calculate SSI^5). Column "$3'$ ex-int" contains number of reads mapped to the exon-intron boundary on the 3'-end of an intron (used to calculate SSI^3).

intron	$5'$ ex-int	$3'$ ex-int	ex-ex	magnitude	*p*-value
1	2463	261	3768	0.03	0
2	679	1465	2100	0.14	6.08e-66
3	1202	1452	6821	0.08	1.32e-06
4	712	1571	10189	0.03	7.54e-74
5	769	1406	9705	0.04	6.09e-43
6	2125	940	17086	0.03	4.19e-104
7	324	1667	5493	0.03	3.13e-217
8	574	409	7064	0.03	1.58e-07
9	1034	1894	12403	0.04	1.46e-57
10	2032	3088	20646	0.05	1.54e-49
11	1840	82	12225	0.01	0
12	880	2660	14853	0.03	1.45e-205
13	**7783**	**9550**	**7525**	**0.34**	**4.29e-41**
14	1935	3046	18715	0.05	3.44e-56
15	8137	4099	30855	0.06	4.23e-297
16	4602	3264	11903	0.12	1.36e-51
17	786	2272	14427	0.03	1.15e-165

Table S3: Representation of recursive splicing events (column "coordinates") in the captured dataset. All detected events are located on chromosome 3.

Coordinates	Splice site	N1	N2	N3	N4
180,653,019-180,665,633	acceptor	1	1	4	1
180,674,213-180,675,607	donor	2	2	4	2
180,674,835-180,675,607	donor	5	4	2	1
180,680,878-180,681,592	acceptor	5	1	4	2
180,686,042-180,687,934	acceptor	20	73	42	23
180,688,146-180,688,665	acceptor	8	401	85	29
180,689,975-180,692,201	both	5	9	10	3
180,692,935-180,693,101	donor	13	37	26	18

Table S4: Canonical and non-canonical splice sites in potential recursive splicing events.

Number of samples	Non-annotated acceptor		Non-annotated donor	
containing an event	number of events	AGxx	number of events	xxGT
Five out of five	4	75%	3	100%
Four out of five	36	86%	28	100%
Three out of five	53	90%	49	100%
Two out of five	78	85%	95	95%

Table S5: Representation of recursive splicing in *TIA1* detected in the non-targeted dataset. Column "coordinates" contains the coordinates of recursive splicing events in on the reference genome. Column "splice site" indicates which splice site is non-annotated. Columns "C1", "C2" and "U1" contain the number of reads supporting each recursive splicing event in each RNA sample from the non-targeted dataset.

Coordinates	Splice site	C1	C2	U1
70,443,631-70,443,885	donor	15	3	61
70,451,761-70,452,460	donor	16	5	7
70,451,761-70,452,597	donor	1	1	1
70,452,525-70,454,867	acceptor	15	3	17
70,454,954-70,455,476	donor	23	15	16
70,455,594-70,456,191	acceptor	20	20	13
70,457,986-70,460,773	donor	4	3	6
70,460,894-70,463,211	acceptor	1	1	2
70,463,307-70,465,921	donor	5	2	2
70,469,796-70,469,830	both	5	3	2

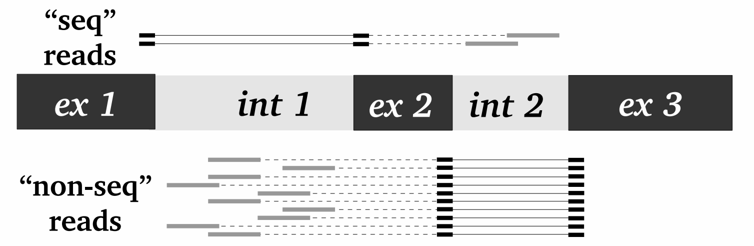

Figure S1: Read pairs supporting sequential ("seq") or non-sequential ("non-seq") splicing. Thick black lines represent ends that were split over a junction (and the thin black line connects the pieces from one end of a read pair). Thick gray lines represent ends mapped to the introns. Dashed line connects two ends of one read pair. In this example, number of "non-seq" read pairs equals 10 and the number of "seq" reads equals 2.

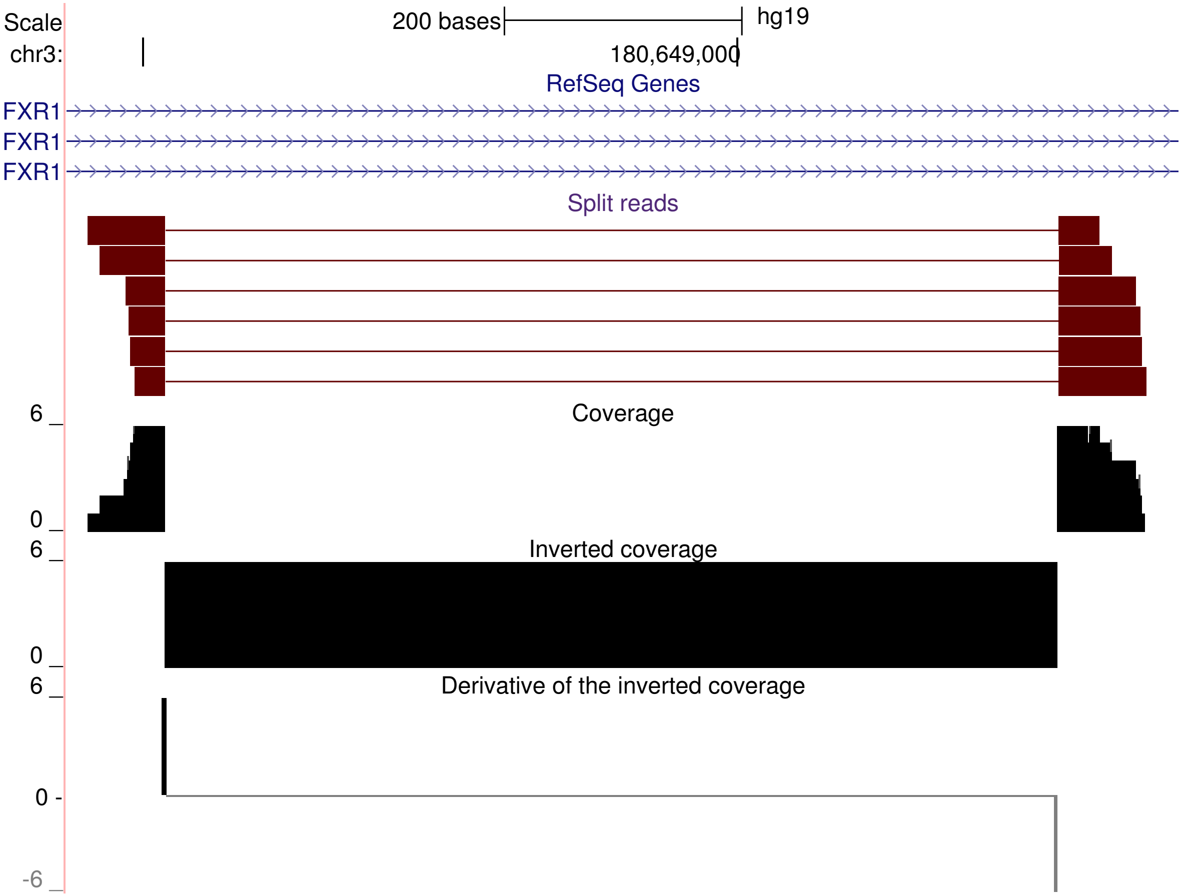

Figure S2: Schematic representation of the recursive splicing analysis. A split read (not mapped to an exon-exon junction) is used to calculate the inverted coverage. The derivative of the inverted coverage is then calculated, producing peaks at the positions where the split starts and drops at the positions where split ends. The size of peaks and drops equals the amount of reads split at this position.

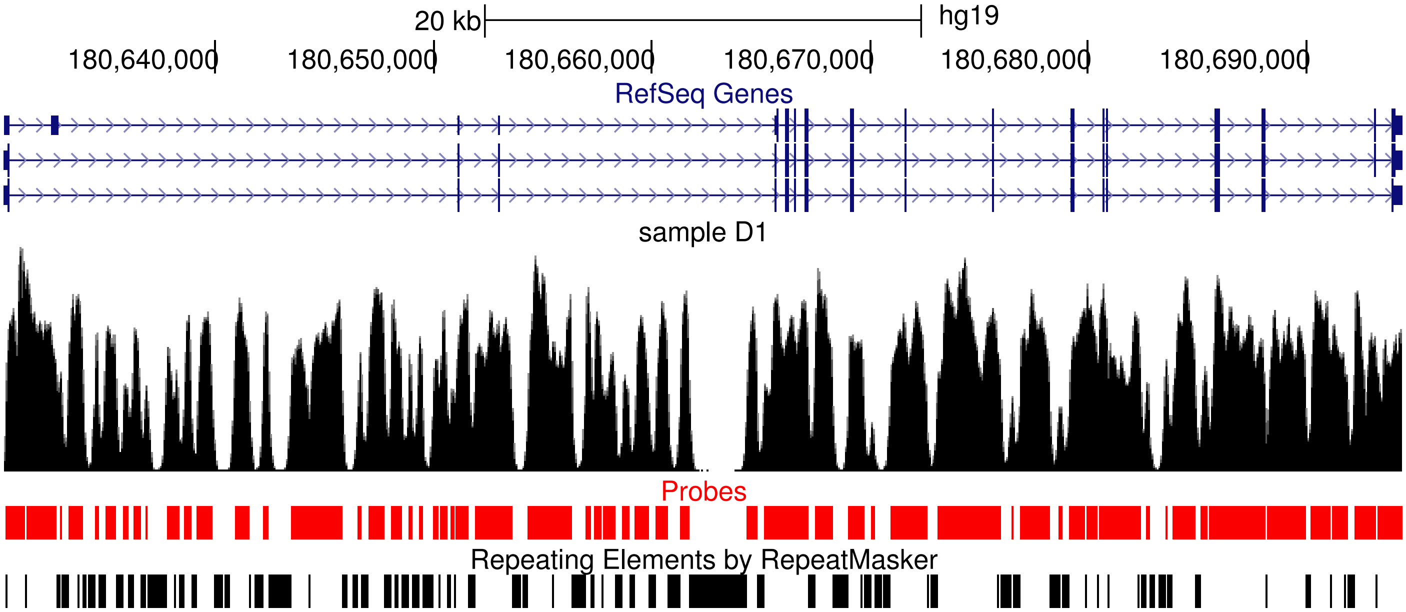

Figure S3: Overview of the coverage across the whole gene being evenly distributed across exons and introns. Coverage of exons and introns in the DNA sample and its correlation with the probes and Repeat Masker regions. Top panel ("RefSeq Genes") indicates the NCBI annotation of the *FXR1* gene used for the analysis, thick blocks depicting exons and thin lines with arrows depicting introns. Second panel ("sample D1") shows the coverage of the DNA sample from the captured dataset (y-axis reflects the coverage, maximum coverage being over 2000). Third panel in red ("Probes") reflects the areas that have been covered by probes (blank areas depict the regions where no probes have been designed). The bottom panel ("Repeating Elements by Repeat Masker") indicate the Repeat Masker track provided by UCSC that has been used to design the probes (black areas depict repetitive elements that were not included in the probes).

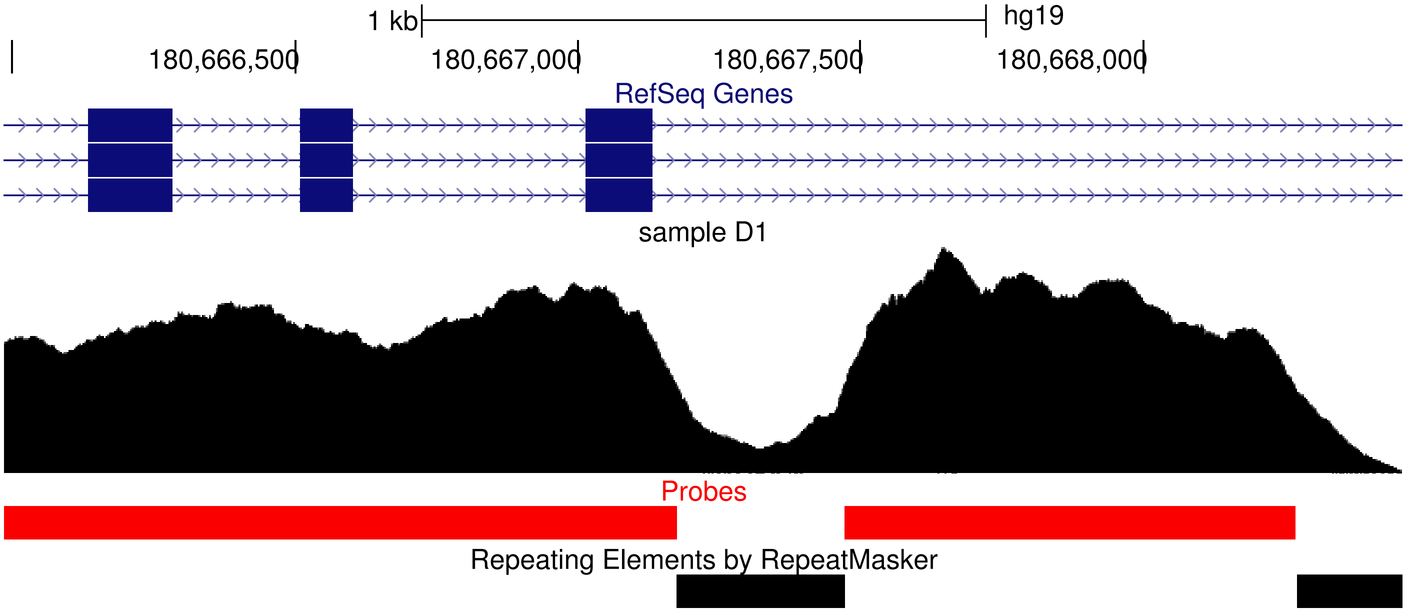

Figure S4: Zoomed-in overview of the coverage, showing no difference between the coverage distribution across an exon and an intron.

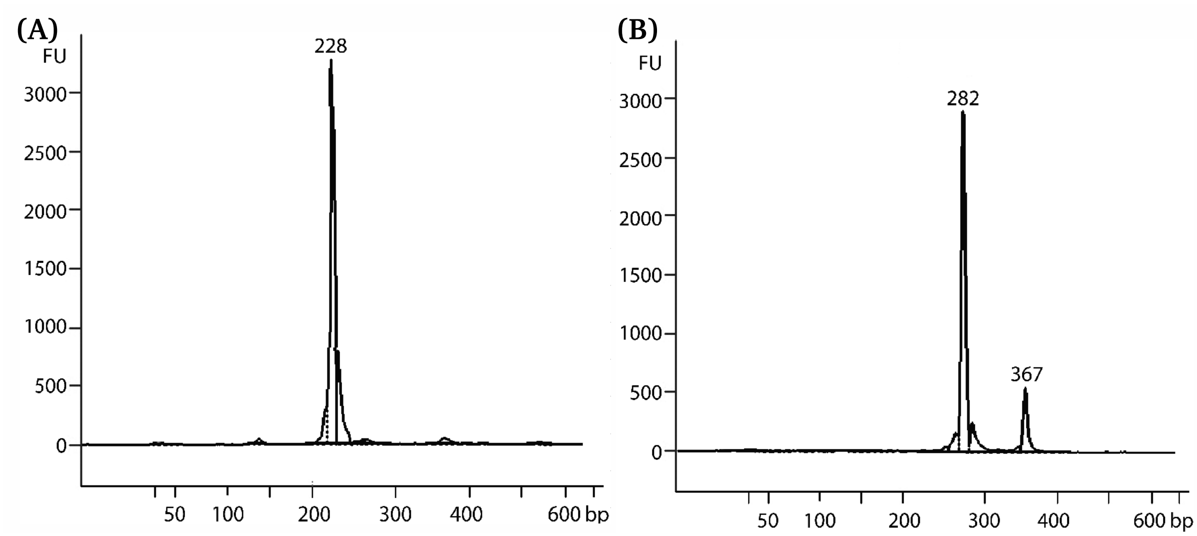

Figure S5: The results of PCR amplification experiments proving a skip of exon 2 and a retention of intron 13 in *FXR1*, as predicted *in silico* by the pipeline. **A.** PCR primers were designed to anneal to exon 1 and exon 5, and this fragment was amplified. The highest peak indicates a fragment of exon 1-exon 5 without exon 2 (228 bp in length). The abundance of transcripts containing exon 2 is very low and the fragment containing exon 2 (571 bp) is not visible. **B.** PCR primers were designed to anneal to exon 12 and exon 15, and the targeted fragments were amplified. The lower peak indicates a fragment with intron 13 inclusion (367 bp in length). The higher peak indicates a fragment without intron 13 (282 bp in length).

Calculating magnitude and likelihood for each intron of a gene in order to estimate its probability to be retained. *"M"* stands for "magnitude" and *"p-value"* stands for the *p*-value of the binomial test for likelihood:

$$M = \frac{min(ex\text{-}int_1,\ ex\text{-}int_2)}{min(ex\text{-}int_1,\ ex\text{-}int_2) + ex\text{-}ex} \tag{2.3}$$

$$p\text{–}value = p\text{-}value_{binom}(ex\text{-}int_1,\ ex\text{-}int_2,\ 0.5) < 0.05 \tag{2.4}$$

```
   1  ATGGCGGAGC TGACGGTGGA GGTTCGCGGC TCTAACGGGG CTTTCTACAA  50
  51  GGGATTTATC AAAGATGTTC ATGAAGACTC CCTTACAGTT GTTTTTGAAA  100
 101  ATAATTGGCA ACCAGAACGC CAGGTTCCAT TTAATGAAGT TAGATTACCA  150
 151  CCACCACCTG ATATAAAAAA AGAAATTAGT GAAGGAGATG AAGTAGAGGT  200
 201  ATATTCAAGA GCAAATGACC AAGAGCCATG TGGGTGGTGG TTGGCTAAAG  250
 251  TTCGGATGAT GAAAGGAGAA TTTTATGTCA TTGAATATGC TGCTTGTGAC  300
 301  GCTACTTACA ATGAAATAGT CACATTTGAA CGACTTCGGC CTGTCAATCA  350
 351  AAATAAAACT GTCAAAAAAA ATACCTTCTT TAAATGCACA GTGGATGTTC  400
 401  CTGAGGATTT GAGAGAGGCG TGTGCTAATG AAAATGCACA TAAAGATTTT  450
 451  AAGAAAGCAG TAGGAGCATG CAGAATTTTT TACCATCCAG AAACAACACA  500
 501  GCTAATGATA CTGTCTGCCA GTGAAGCAAC TGTGAAGAGA GTAAACATCT  550
 551  TAAGTGACAT GCATTTGCGA AGTATTCGTA CGAAGTTGAT GCTTATGTCC  600
 601  AGAAATGAAG AGGCCACTAA GCATTTAGAA TGCACAAAAC AACTTGCAGC  650
 651  AGCTTTTCAT GAGGAATTTG TTGTGAGAGA AGATTTAATG GGCCTGGCAA  700
 701  TAGGAACACA TGGTAGTAAC ATCCAGCAAG CTAGGAAGGT TCCTGGAGTT  750
 751  ACCGCCATTG AGCTAGATGA AGATACTGGA ACATTCAGAA TCTACGGAGA  800
 801  GAGTGCTGAT GCTGTAAAAA AGGCTAGAGG TTTCTTGGAA TTTGTGGAGG  850
 851  ATTTTATTCA GGTTCCTAGG AATCTCGTTG GAAAAGTAAT TGGAAAAAAT  900
 901  GGCAAAGTTA TTCAAGAAAT AGTGGACAAA TCTGGTGTGG TTCGAGTGAG  950
 951  AATTGAAGGG GACAATGAAA ATAAATTACC CAGAGAAGAC GGTATGGTTC  1000
1001  CATTTGTATT TGTTGGCACT AAAGAAAGCA TTGGAAATGT GCAGGTTCTT  1050
1051  CTAGAGTATC ATATTGCCTA TCTAAAGGAA GTAGAACAGC TAAGAATGGA  1100
1101  ACGCCTACAG ATTGATGAAC AGCTGCGACA GATTGGTTCT AGGTCTTATA  1150
1151  GCGGAAGAGG CAGAGGTCGT CGGGGACCTA ATTACACCTC CGGTTATGGT  1200
1201  ACAAATTCTG AGCTGTCTAA CCCCTCTGAA ACGGAATCTG AGCGTAAAGA  1250
1251  CGAGCTGAGT GATTGGTCAT TGGCAGGAGA AGATGATCGA GACAGCCGAC  1300
1301  ATCAGCGTGA CAGCAGGAGA CGCCCAGGAG GAAGAGGCAG AAGTGTTTCA  1350
1351  GGGGGTCGAG GTCGTGGTGG ACCACGTGGT GGCAAATCCT CCATCAGTTC  1400
1401  TGTGCTCAAA GATCCAGACA GCAATCCATA CAGCTTACTT GATAATACAG  1450
1451  AATCAGATCA GACTGCAGAC ACTGATGCCA GCGAATCTCA TCACAGTACT  1500
1501  AACCGTCGTA GGCGGTCTCG TAGACGAAGG ACTGATGAAG ATGCTGTTCT  1550
1551  GATGGATGGA ATGACTGAAT CTGATACAGC TTCAGTTAAT GAAAATGGGC  1600
1601  TAGATGATAG TGAAAAAAAA CCCCAGCGAC GCAATCGTAG CCGCAGGCGT  1650
1651  CGCTTCAGGG GTCAGGCAGA AGATAGACAG CCAGTCACAG TTGCAGATTA  1700
1701  TATTTCTAGA GCTGAGTCTC AGAGCAGACA AAGAAACCTC CCAAGGGAAA  1750
1751  CTTTGGCTAA AAACAAGAAA GAAATGGCAA AAGATGTGAT TGAAGAGCAT  1800
1801  GGTCCTTCAG AAAAGGCAAT AAACGGCCCA ACTAGTGCTT CTGGCGATGA  1850
1851  CATTTCTAAG CTACAGCGTA CTCCAGGAGA AGAAAAGATT AATACCTTAA  1900
1901  AAGAAGAAAA CACTCAAGAA GCAGCAGTCC TGAATGGTGT TTCATAA     1947
```

Figure S6: Novel exon (in red) predicted by the pipeline and its location in the full-length *FXR1* transcript. The exon is located between exons 16 and 17 (according to the annotation used in this paper). The full-length transcript has been experimentally validated by Sanger sequencing.

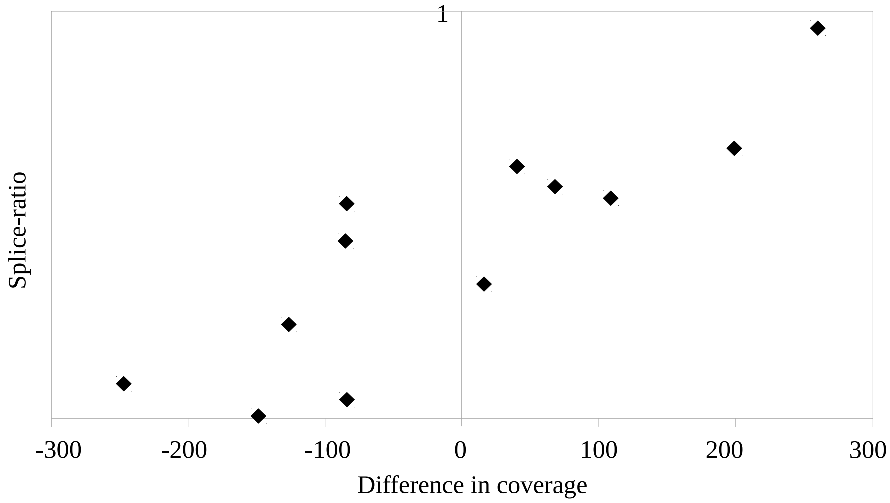

Figure S7: Linear correlation between the difference in median coverage ($\text{intron}_{i+1} - \text{intron}_i$) and the splice ratio. Correlation shown for the pre-mRNA N1 sample. Pearson correlation: -0.86. Spearman correlation: -0.84.

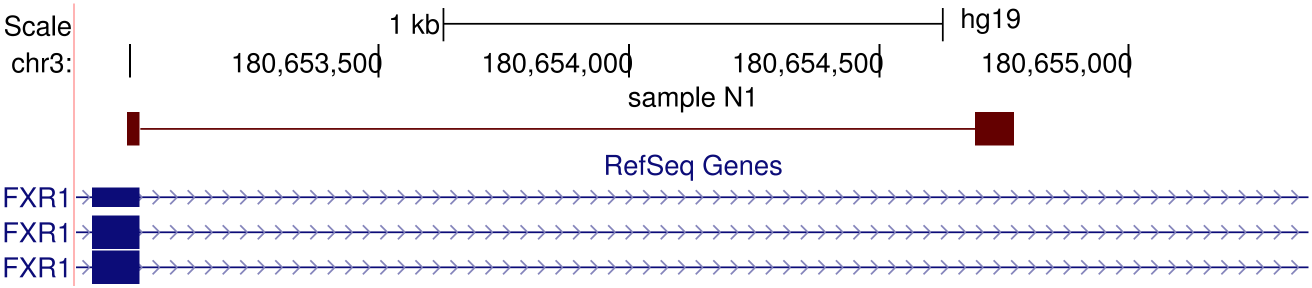

Figure S8: Example of a recursive splicing event happening on the 5' end of intron 14.

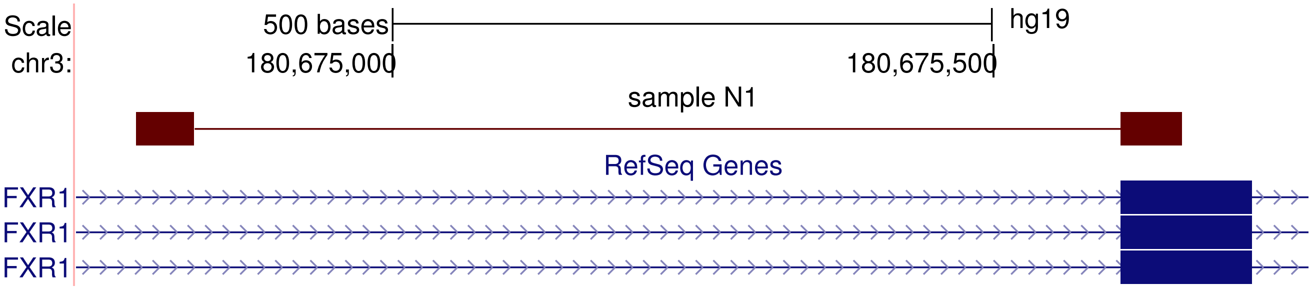

Figure S9: Example of a recursive splicign event happening on the 3' end of intron 10.

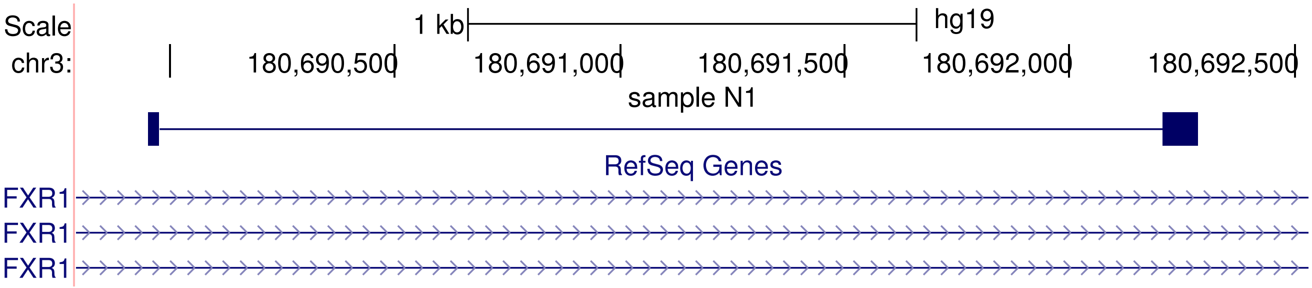

Figure S10: Example of recursive splicing with two non-canonical splice sites in intron 16.

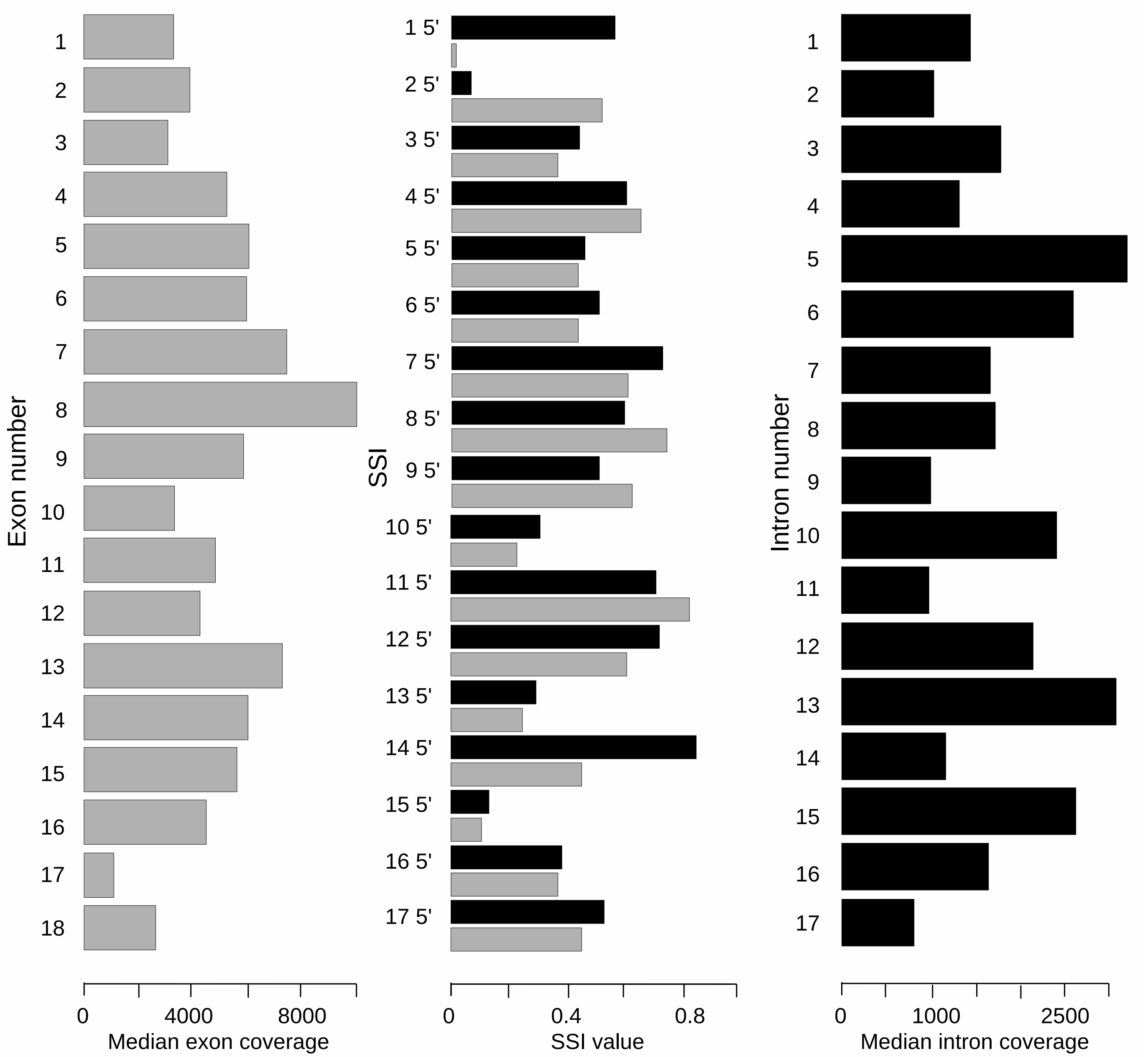

Figure S11: Splice site index (SSI) and medians of coverage of exons and introns in *FXR1* for sample C1 from the ENCODE dataset. Gray bars in the left panel represent the coverage of exons (exon 1 on top). Black bars in the middle panel represent SSI values for the 5' end of the introns and gray bars on the middle panel represent SSI values for the 3' end of the introns (intron 1 on top). Black bars in the right panel represent the coverage of introns (intron 1 on top). Data shown for chromatin RNA sample C2.

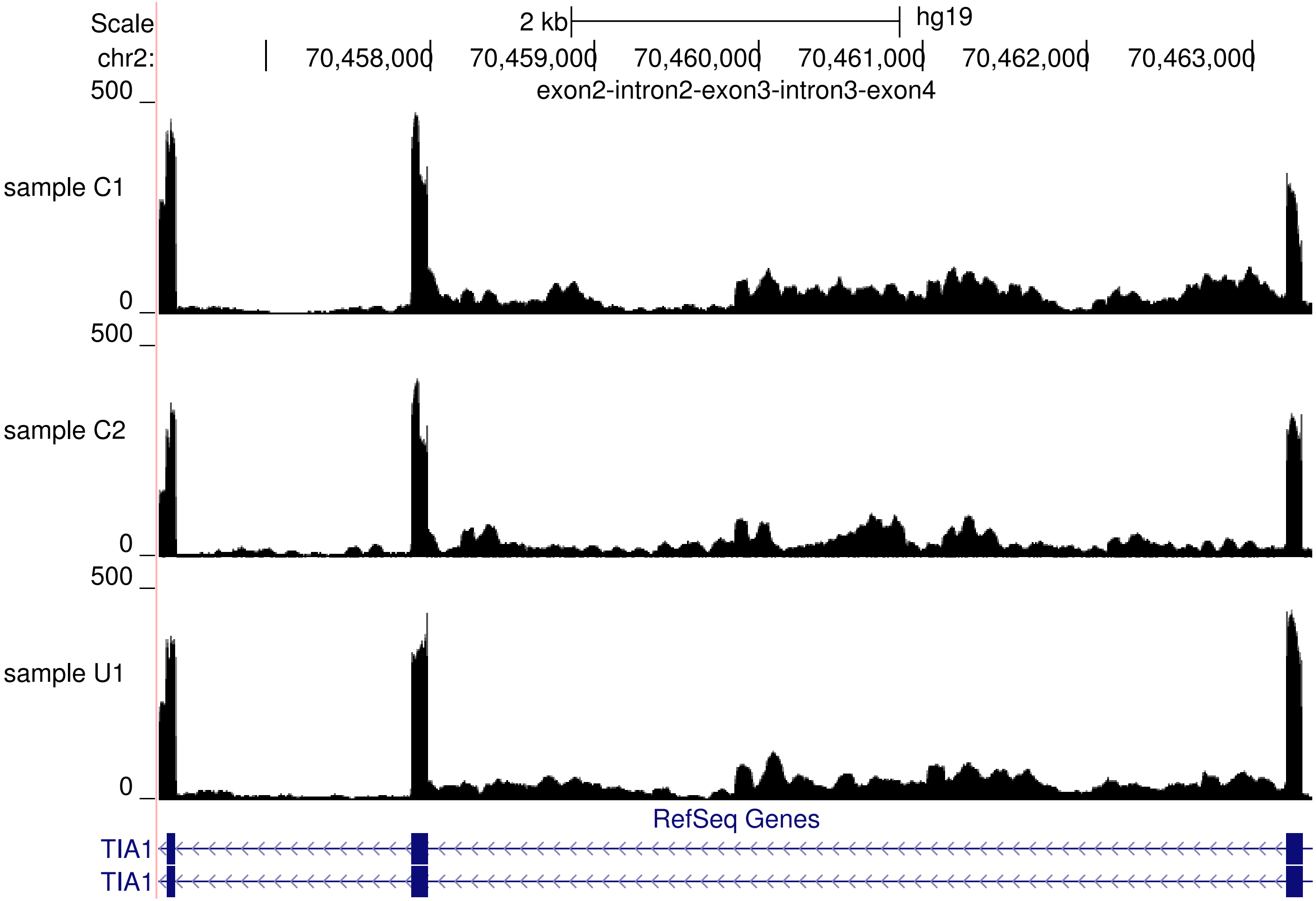

Figure S12: Graphical representation of two potentially non-sequentially spliced introns of *TIA1* – intron 2 is predicted to be spliced after intron 3. Top three panels represent the coverage from samples N1, N2 and U1. Coverage is the value on the y-axis, and the genomic coordinates are the value on the x-axis. The bottom panel represents the annotation of the gene available in the RefSeq database. Thick blocks represent exons, thin lines with arrows represent introns. Note that the gene is transcribed from the reverse strand and on the figure intron 2 is situated downstream (on the right) from intron 3. None of the introns with high coverage are annotated as retained introns, which gives an extra evidence that this is a case of non-sequential splicing and not a case of intron retention.